

# Anisotropic modeling of short fibers reinforced thermoplastics materials with LS-DYNA

Alexandre Hatt<sup>1</sup>

<sup>1</sup>Faurecia Automotive Seating, Simplified Limited Liability Company

## 1 Abstract / Summary

Polymer thermoplastics materials are widely used in the automotive industry with the injection molding process. For structural applications, the most common reinforcement is to add discontinuous short glass fibers to increase the stiffness and the mechanical properties.

Due to the aspect ratio of the fibers and the fiber orientation inside the material, the mechanical properties of the reinforced polymer will become anisotropic. The injection molding process will orient the fibers regarding the material flow inside the mold during the filling phase.

With injection molding simulation tools, the fiber orientation is one of the key outputs that can be used for the structural product simulation.

Faurecia has developed a mapping tool to transfer mold filling fiber orientation results into LS-Dyna structural mesh for the product simulation.

Each elements, each integration points over the thickness is oriented according fiber directions of the mold filling simulation results and some specific anisotropic linear elastic / nonlinear viscoplastic mechanical properties are affected according fiber orientation tensors results.

Anisotropic characterization of the composite material associated with composite homogenization simulations is used to fill the different mechanical properties of the fiber orientation discretization.

The fiber reinforced thermoplastic is discretized into several \*MAT\_ANISOTROPIC\_ELASTIC\_PLASTIC regarding different fiber orientation tensors possibilities, from a diffuse isotropic fiber orientation to a highly orthotropic fiber orientation.

Failure criteria are integrated with the \*MAT\_ADD\_EROSION features with the same fiber orientation tensor discretization as for the \*MAT\_ANISOTROPIC\_ELASTIC\_PLASTIC. The use of maximum stress and strain versus strain rate and triaxiality is used to modelize rupture under crash solicitations and fiber orientation.

Validations and correlations have been performed on a PA6 I GF35 reference beam under static and dynamic three points bending.

## 2 Rheology simulation and fiber orientation mapping process

The mold filling simulation will predict the material flow inside the mold regarding material viscosity, temperature, pressure, and shear rate. The fibers are aligned according to the flow orientation. The simulation is using Folgar-Tucker equation to estimate fiber orientation regarding material flow.

One of the key outputs for this process simulation will be the fiber orientation for each element, each integration point over the thickness (12 layers over thickness in general). The fiber orientation is written in an ascii file in a tensor format.

The fiber orientation results are visualized with sized colored vectors indicating the three principal directions of the fibers. The biggest vector is the major principal direction with an associated color which is indicating the ratio of fibers oriented in the major principal fiber direction. The second and third principal fiber directions are orthogonal to the first direction with specific fiber ratio for each.

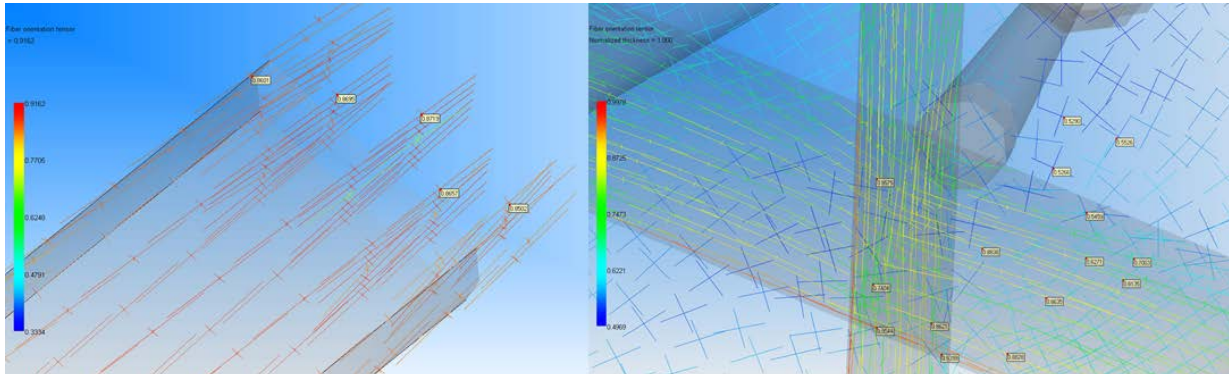


Fig.1: Principal fiber orientation with fibers highly oriented in the major direction (left) and with mixed orientations between the two principal's directions (right)

Faurecia has developed a mapping tool that will orient every element and every thickness integration point of the LS-Dyna structural mesh regarding the major principal fiber direction.

Some specific \*MAT\_ANISOTROPIC\_ELASTIC\_PLASTIC anisotropic nonlinear elastoviscoplastic material models are affected for each integration point over the thickness regarding the fiber ratio between the principals fibers directions.

The material is oriented according the major principal fiber direction with aopt=0 (material axis oriented according element nodes) with a \*PART\_COMPOSITE for each element indicating the material ID per layer, the layer thickness, and the layer orientation according to the major fiber direction.

See example below for one element:

```
*PART_COMPOSITE
POUTRE_PLASTIQUE_1_030209_TOP_RO_RIB_2.4_PROP1000
$#      pid      elform      shrf      nloc      marea      hgid      adpopt      ithelfrm
      1000         16         0         0         0         0         0         0
$#      mid1     thick1      b1      ithid1     mid2     thick2      b2      ithid2
      1006     0.144     0.00         0         1006     0.170     -1.00         0
      1006     0.193     -4.00         0         1006     0.214     -6.00         0
      1006     0.232     -5.00         0         1007     0.247     4.00         0
      1007     0.247     4.00         0         1006     0.232     -5.00         0
      1006     0.214     -6.00         0         1006     0.193     -4.00         0
      1006     0.170     -1.00         0         1006     0.144     0.00         0
*ELEMENT_SHELL_BETA
$#      eid      pid      n1      n2      n3      n4      n5      n6      n7      n8
      1041799    1000  1040073  1040273  1040279  1040063      0      0      0      0
$#      thic1      thic2      thic3      thic4      psi
      2.400      2.400      2.400      2.400      0
```

### 3 Composite homogenization and material orientation discretization

A specific anisotropic material characterization is required with coupons cut into one side injection gate plates. The coupons are cut with 0°, 45°, and 90° angles versus material flow. The fiber orientation inside the plate is measured by tomography to know exactly the microstructure fiber orientation for the tensile tests.

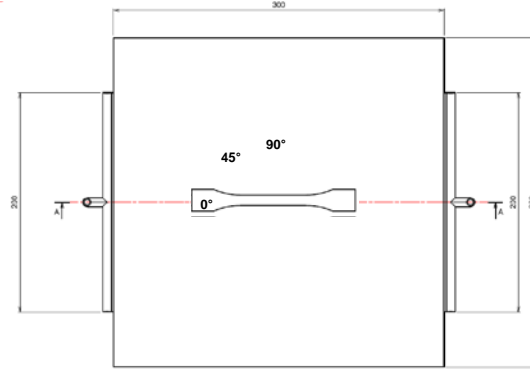


Fig.2: One side injected plate to cut tensile coupons

Tensile tests are performed at different strain rate (0.001/sec to 100/sec). The results will be used to create two different microstructural material models:

- Isotropic nonlinear elastoviscoplastic for the thermoplastic matrix
- Isotropic linear elastic for the glass fibers

The identification of the material parameters is done by reverse engineering to fit the tests results with a homogenization method (Digimat or with a 3D representative volume element).

Once the two micro-material models are created, some tensile simulations with different fiber orientation tensors will be performed to export anisotropic flow curves.

The composite material will be discretized regarding fiber orientation from an isotropic material with an average fiber orientation between the principal directions until a highly orthotropic material with 100% of the fibers in the major principal direction.

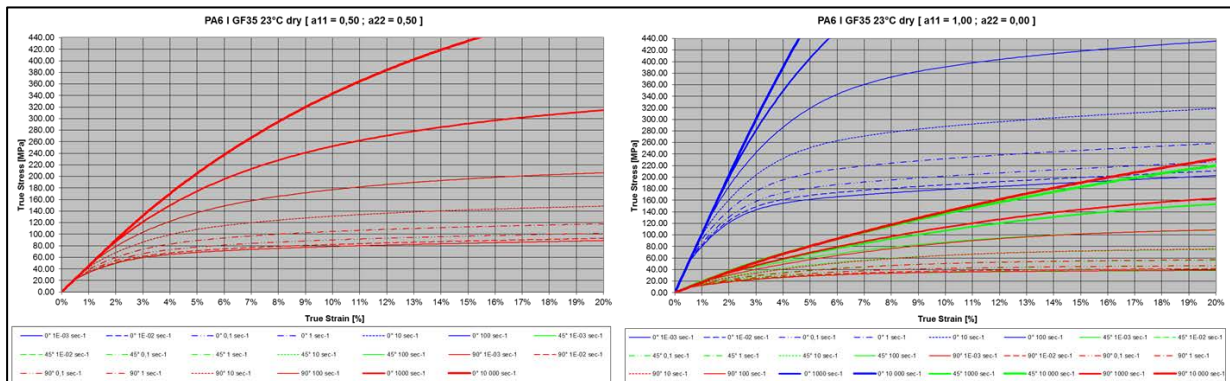


Fig.3: Flow curve export with average fiber orientation (50% of fibers in 0° and 90°, left) and highly oriented fibers (100 % of the fibers in 0°, right)

The material fiber orientation discretization has been setup every 5% of the fiber orientation tensor which is also defined in the mapping tool to affect the same material properties regarding fiber orientation distribution between the principal directions. For shell elements with 5% of fiber orientation tensor discretization, the total number of \*MAT\_ANISOTROPIC\_ELASTIC\_PLASTIC will be eleven:

$$\begin{bmatrix} a_{11} = 0,50 & a_{12} = 0 & a_{13} = 0 \\ a_{21} = 0 & a_{22} = 0,50 & a_{23} = 0 \\ a_{31} = 0 & a_{32} = 0 & a_{33} = 0 \end{bmatrix}, 
 \begin{bmatrix} a_{11} = 0,55 & a_{12} = 0 & a_{13} = 0 \\ a_{21} = 0 & a_{22} = 0,45 & a_{23} = 0 \\ a_{31} = 0 & a_{32} = 0 & a_{33} = 0 \end{bmatrix}, 
 \begin{bmatrix} a_{11} = 0,60 & a_{12} = 0 & a_{13} = 0 \\ a_{21} = 0 & a_{22} = 0,40 & a_{23} = 0 \\ a_{31} = 0 & a_{32} = 0 & a_{33} = 0 \end{bmatrix}, \\
 \begin{bmatrix} a_{11} = 0,65 & a_{12} = 0 & a_{13} = 0 \\ a_{21} = 0 & a_{22} = 0,35 & a_{23} = 0 \\ a_{31} = 0 & a_{32} = 0 & a_{33} = 0 \end{bmatrix}, 
 \begin{bmatrix} a_{11} = 0,70 & a_{12} = 0 & a_{13} = 0 \\ a_{21} = 0 & a_{22} = 0,30 & a_{23} = 0 \\ a_{31} = 0 & a_{32} = 0 & a_{33} = 0 \end{bmatrix}, 
 \begin{bmatrix} a_{11} = 0,75 & a_{12} = 0 & a_{13} = 0 \\ a_{21} = 0 & a_{22} = 0,25 & a_{23} = 0 \\ a_{31} = 0 & a_{32} = 0 & a_{33} = 0 \end{bmatrix},$$

$$\begin{bmatrix} a_{11} = 0,80 & a_{12} = 0 & a_{13} = 0 \\ a_{21} = 0 & a_{22} = 0,20 & a_{23} = 0 \\ a_{31} = 0 & a_{32} = 0 & a_{33} = 0 \end{bmatrix}, \begin{bmatrix} a_{11} = 0,85 & a_{12} = 0 & a_{13} = 0 \\ a_{21} = 0 & a_{22} = 0,15 & a_{23} = 0 \\ a_{31} = 0 & a_{32} = 0 & a_{33} = 0 \end{bmatrix}, \begin{bmatrix} a_{11} = 0,90 & a_{12} = 0 & a_{13} = 0 \\ a_{21} = 0 & a_{22} = 0,10 & a_{23} = 0 \\ a_{31} = 0 & a_{32} = 0 & a_{33} = 0 \end{bmatrix},$$

$$\begin{bmatrix} a_{11} = 0,95 & a_{12} = 0 & a_{13} = 0 \\ a_{21} = 0 & a_{22} = 0,05 & a_{23} = 0 \\ a_{31} = 0 & a_{32} = 0 & a_{33} = 0 \end{bmatrix}, \begin{bmatrix} a_{11} = 1,00 & a_{12} = 0 & a_{13} = 0 \\ a_{21} = 0 & a_{22} = 0,00 & a_{23} = 0 \\ a_{31} = 0 & a_{32} = 0 & a_{33} = 0 \end{bmatrix}$$

#### 4 LS-Dyna anisotropic elastoviscoplastic material model \*MAT\_ANISOTROPIC\_ELASTIC\_PLASTIC

Dynamore developed some new features of the \*MAT\_ANISOTROPIC\_ELASTIC\_PLASTIC to integrate strain rate sensitivity for anisotropic plasticity with VP=1 option (LS-Dyna Dev 88716).

The \*MAT\_ANISOTROPIC\_ELASTIC\_PLASTIC (\*MAT\_157) is a combination of the \*MAT\_ANISOTROPIC\_ELASTIC (\*MAT\_002\_ANIS) which is the anisotropic stiffness matrix with the \*MAT\_ANISOTROPIC\_VISCOPLASTIC (\*MAT\_103\_P) which is isotropic linear elastic and anisotropic nonlinear viscoplastic.

So the \*MAT\_ANISOTROPIC\_ELASTIC\_PLASTIC (\*MAT\_157) is:

- Anisotropic linear elastic
  - Anisotropic stiffness matrix (36 parameters reduced to 21 with symmetry) :  $\sigma_{ij} = C_{ijkl}\epsilon_{kl}$

$$\begin{pmatrix} \sigma_{11} \\ \sigma_{22} \\ \sigma_{33} \\ \sigma_{12} \\ \sigma_{23} \\ \sigma_{31} \end{pmatrix} = \begin{bmatrix} C_{11} & C_{12} & C_{13} & C_{14} & C_{15} & C_{16} \\ C_{21} & C_{22} & C_{23} & C_{24} & C_{25} & C_{26} \\ C_{31} & C_{32} & C_{33} & C_{34} & C_{35} & C_{36} \\ C_{41} & C_{42} & C_{43} & C_{44} & C_{45} & C_{46} \\ C_{51} & C_{52} & C_{53} & C_{54} & C_{55} & C_{56} \\ C_{61} & C_{62} & C_{63} & C_{64} & C_{65} & C_{66} \end{bmatrix} \begin{pmatrix} \epsilon_{11} \\ \epsilon_{22} \\ \epsilon_{33} \\ \epsilon_{12} \\ \epsilon_{23} \\ \epsilon_{31} \end{pmatrix}$$

- For Orthotropic materials (fibers reinforced plastics), the stiffness matrix is reduced to 9 parameters :

$$\begin{pmatrix} \sigma_{11} \\ \sigma_{22} \\ \sigma_{33} \\ \sigma_{12} \\ \sigma_{23} \\ \sigma_{31} \end{pmatrix} = \begin{bmatrix} C_{11} & C_{12} & C_{13} & 0 & 0 & 0 \\ C_{12} & C_{22} & C_{23} & 0 & 0 & 0 \\ C_{13} & C_{23} & C_{33} & 0 & 0 & 0 \\ 0 & 0 & 0 & C_{44} & 0 & 0 \\ 0 & 0 & 0 & 0 & C_{55} & 0 \\ 0 & 0 & 0 & 0 & 0 & C_{66} \end{bmatrix} \begin{pmatrix} \epsilon_{11} \\ \epsilon_{22} \\ \epsilon_{33} \\ \epsilon_{12} \\ \epsilon_{23} \\ \epsilon_{31} \end{pmatrix}$$

$$\begin{pmatrix} \sigma_{11} \\ \sigma_{22} \\ \sigma_{33} \\ \sigma_{12} \\ \sigma_{23} \\ \sigma_{31} \end{pmatrix} = \begin{bmatrix} \frac{1-\nu_{23}\nu_{32}}{E_{22}E_{33}\Delta} & \frac{\nu_{21}+\nu_{31}\nu_{23}}{E_{22}E_{33}\Delta} & \frac{\nu_{31}+\nu_{21}\nu_{32}}{E_{22}E_{33}\Delta} & 0 & 0 & 0 \\ \frac{\nu_{12}+\nu_{13}\nu_{32}}{E_{11}E_{33}\Delta} & \frac{1-\nu_{13}\nu_{31}}{E_{11}E_{33}\Delta} & \frac{\nu_{32}+\nu_{12}\nu_{31}}{E_{11}E_{33}\Delta} & 0 & 0 & 0 \\ \frac{\nu_{13}+\nu_{12}\nu_{23}}{E_{11}E_{22}\Delta} & \frac{\nu_{23}+\nu_{13}\nu_{21}}{E_{11}E_{22}\Delta} & \frac{1-\nu_{12}\nu_{21}}{E_{11}E_{22}\Delta} & 0 & 0 & 0 \\ 0 & 0 & 0 & 2G_{12} & 0 & 0 \\ 0 & 0 & 0 & 0 & 2G_{23} & 0 \\ 0 & 0 & 0 & 0 & 0 & 2G_{31} \end{bmatrix} \begin{pmatrix} \epsilon_{11} \\ \epsilon_{22} \\ \epsilon_{33} \\ \epsilon_{12} \\ \epsilon_{23} \\ \epsilon_{31} \end{pmatrix}$$

$$\Delta = \frac{1-\nu_{12}\nu_{21}-\nu_{23}\nu_{32}-\nu_{31}\nu_{13}-2\nu_{12}\nu_{23}\nu_{31}}{E_{11}E_{22}E_{33}}$$

$$-\frac{\nu_{21}}{E_{22}} = -\frac{\nu_{12}}{E_{11}}; -\frac{\nu_{31}}{E_{33}} = -\frac{\nu_{13}}{E_{11}}; -\frac{\nu_{32}}{E_{33}} = -\frac{\nu_{23}}{E_{22}}$$

- Anisotropic nonlinear viscoplastic
  - Tabulated flow curves (True Stress versus Effective Plastic Strain) versus strain rate
  - Anisotropic Hill's parameters R00, R45, R90 (for shell) that will modify the plasticity response for 0°, 45°, 90° angles

This material model is able to simulate anisotropy induced by the short fiber orientation inside the thermoplastic.

The final FEA model integrates the fiber orientation by orienting elements and shell thickness integration points and the anisotropy linked to the fiber repartition between the different fiber principal directions.

The numerical stability is similar to a \*MAT\_PIECEWISE\_LINEAR\_PLASTICITY (\*MAT\_024) with an excellent computation time, 100% under LS-Dyna without any external software coupling. This simulation method is applicable for an industrial / project approach and already deployed at Faurecia.

But some limitations regarding the real material behavior are still done:

- The material is not viscoelastic.
- There is no triaxiality dependency for the flow curves.

## 5 Failure modeling by element erosion: \*MAT\_ADD\_EROSION

The rupture of the fiber reinforced plastic will depend on the following parameters

- Fiber orientation
- Strain rate
- Triaxiality

The material is brittle so the damage function by softening is not used.

\*MAT\_ANISOTROPIC\_ELASTIC\_PLASTIC has no failure criteria included, so \*MAT\_ADD\_EROSION is used to define failure criteria by element erosion.

Two different isotropic failure conditions are applied to represent anisotropic failure:

- Maximum Stress Von Mises for Longitudinal (0° axis) failure versus Strain rate (SIGVM with -LCID)
- Maximum Anisotropic Effective Plastic Strain for transversal (90° axis) failure versus Triaxiality versus Strain rate (IDAM=1, GISSMO with dmgtyp=81)

As the stiffness is much higher for the longitudinal axis, the maximum stress values will not be reached by the transverse axis, and the maximum strain values for the transverse axis will not be reached in the longitudinal axis because the stress at failure will occur before.

If one of the two failure conditions is reached (ncs=1), the thickness integration point fails. If more than 80% of the thickness integration points fail (Faurecia setting), then the element is suppressed.

The \*MAT\_ADD\_EROSION fiber orientation decomposition will follow the same \*MAT\_ANISOTROPIC\_ELASTIC\_PLASTIC decomposition. So if 11 \*MAT\_157 are created, 11 correspondent \*MAT\_ADD\_EROSION will be added.

The maximum stress and strain values are measured by testing and/or composite homogenization simulations.

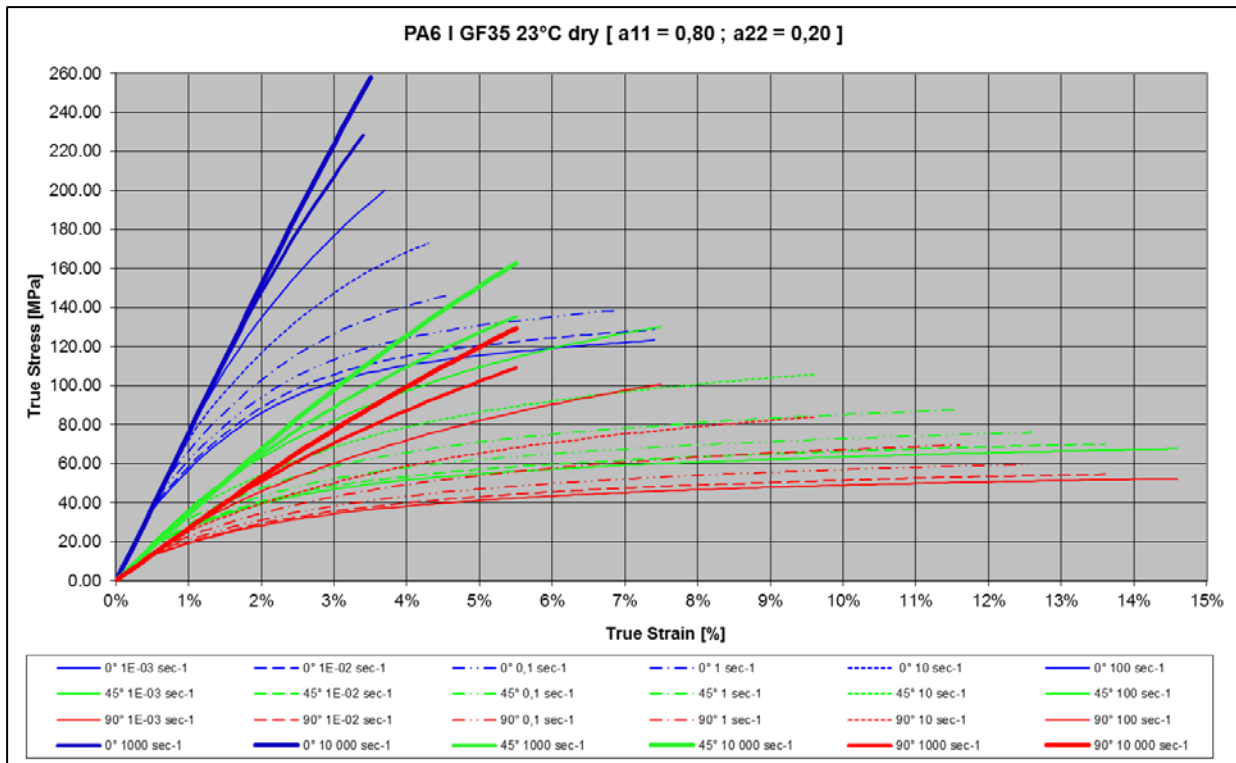


Fig.4: Stress vs Strain Uniaxial tension strain rate dependency with failure (80% of the fibers in 0° and 20% in 90° principal direction)

## 6 Correlation on beams

Static and dynamic three points bending tests have been performed on plastic beams with omega profile and cross ribs inside with different injections gates to have tests results versus injection process configurations.

The beams have been molded with one or three gates injection configuration with a different fiber orientation tensor in the middle / impact area.

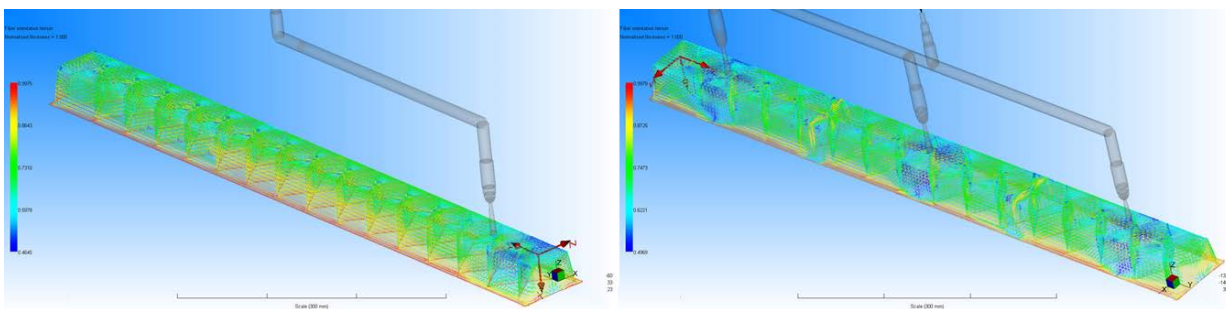


Fig.5: One injection gate (left) / Three injection gates (right) beam fiber orientation results

### 6.1 LS-Dyna anisotropic beam model

The mapping process has been applied to orient elements and anisotropic material (\*MAT\_157) for each molding configurations. The beam FEA model contains:

- 59 303 \*ELEMENT\_SHELL\_BETA
- 54 761 \*PART\_COMPOSITE

- 12 layers oriented according the rheology simulation major principal fiber orientation output
- Elform 16 full integration
- 11 \*MAT\_ANISOTROPIC\_ELASTIC\_PLASTIC with 11 \*MAT\_ADD\_EROSION which corresponds to the composite homogenized material discretization with failure erosion criteria regarding fiber ratio between principals fiber directions

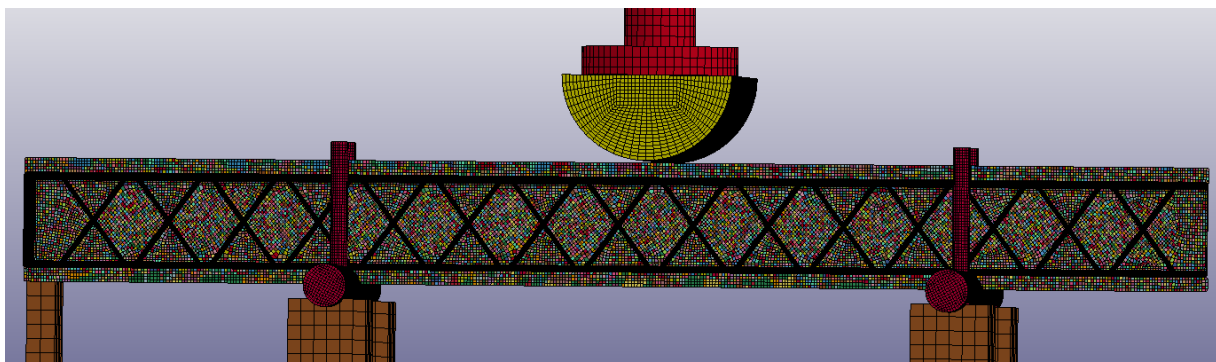


Fig.6: LS-Dyna Dynamic three points bending Faurecia Matcar beam anisotropic elastoviscoplastic model

### 6.2 Static three points bending

The beam profile is placed in a horizontal position, and the impactor has a fixed velocity. Material strain rate sensitivity is removed. The contact force versus the impactor displacement is measured.

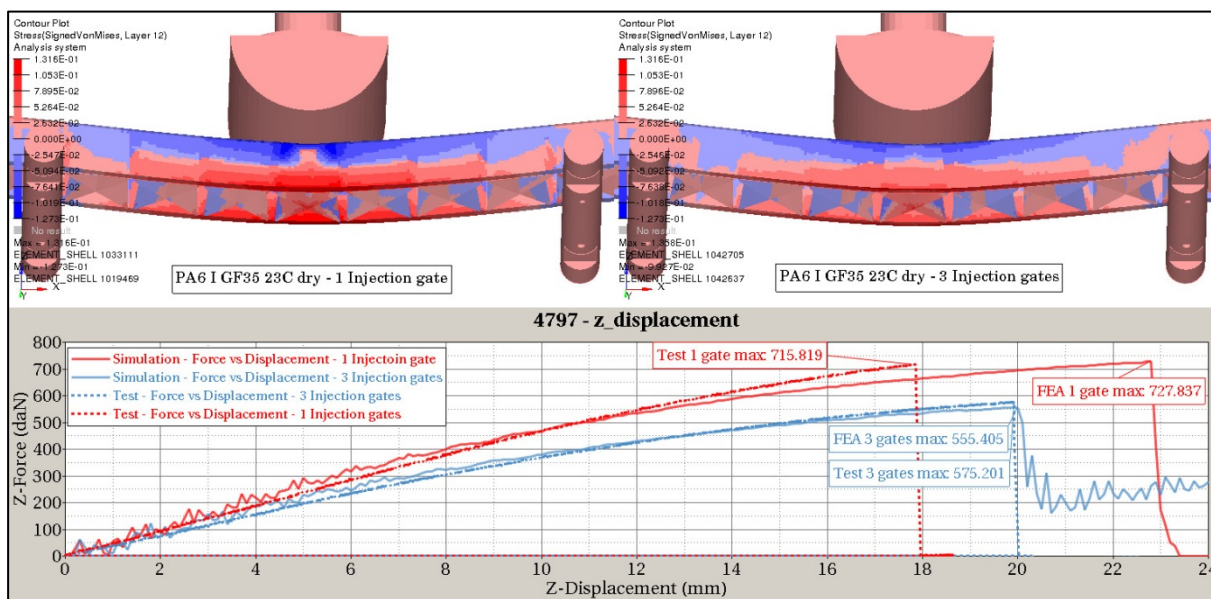


Fig.7: Static three points bending Simulations / Tests results for one and three injection gates (PA6 I GF35 23°C dry)

Simulation and tests results show different results between injection configurations. The beam stiffness is increased for the one injection gate configuration due to a better fiber orientation in the beam length. Simulations and tests are closed for the stiffness and the load at rupture. A difference of 4 mm versus test result is observed for the maximum displacement with one injection gate model.

### 6.3 Dynamic three points bending

The beam profile is placed in vertical position, the drop impactor has an initial velocity of 2,37 m/s with a weight of 55 kg (155 J). Impactor deceleration is measured.



Fig.8: Dynamic three points bending superposition Test / Simulation 1 injection gate (left), 3 injection gates (right)

Simulations and tests results show different results for the one and three injection gates configurations with the same effects. Acceleration values are higher with the three injection gates beam due to higher strain at break in the beam impact area produced by the diffuse fiber orientation. Simulation results are slightly shifted in the time scale with a maximum acceleration peak 2g lower than tests results.

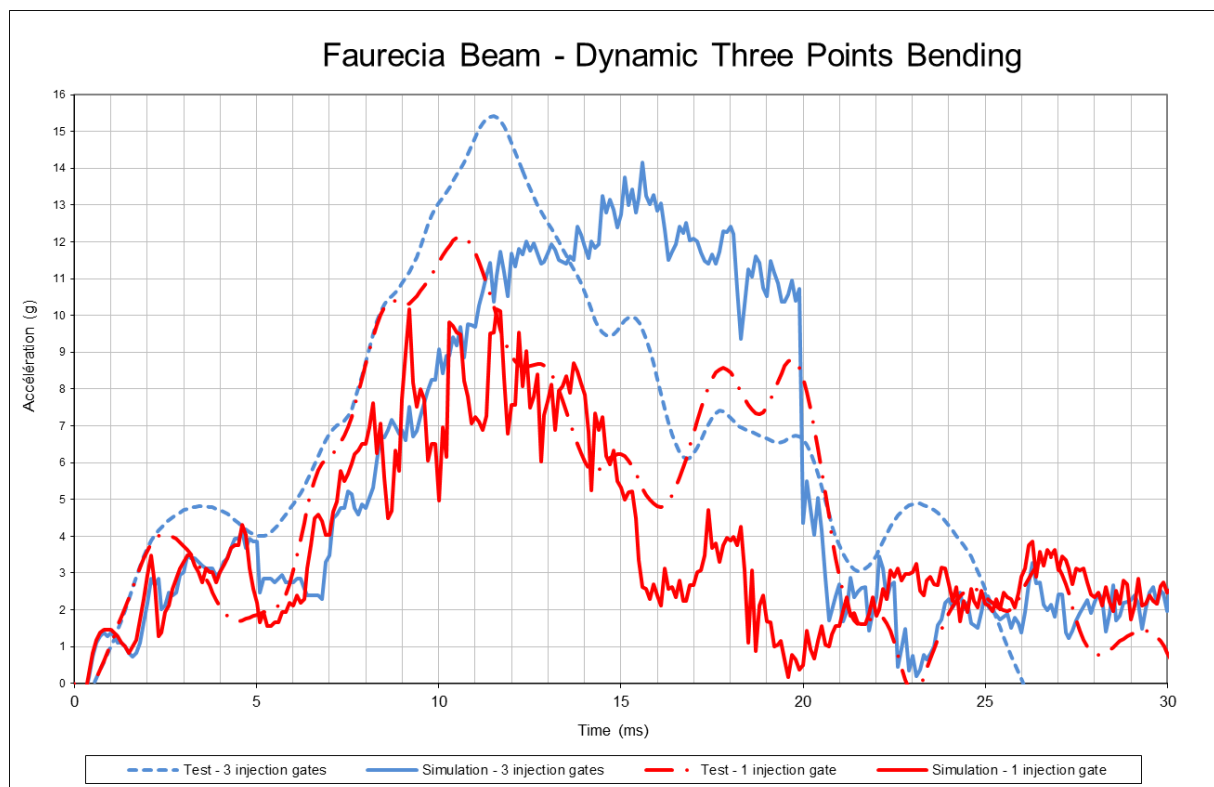


Fig.9: Dynamic three points bending simulations / tests results – Force versus Displacement

Viscoelasticity of the material is not modeled and the beam is progressively damaged by cracks propagations which are mesh dependent and more difficult to simulate.



## 7 Conclusion

Integration of anisotropic injection molding process effect of the short fiber orientation inside thermoplastics materials has been modeled with LS-Dyna \*MAT\_ANISOTROPIC\_ELASTIC\_PLASTIC.

The definition of a mapping tool between process simulation and structural LS-Dyna simulation will define material discretization versus fiber orientation tensor and orient each element and each thickness integration points.

Specific anisotropic material characterizations on injected plates with micro / macro scales homogenizations are required to define material decomposition regarding fiber orientation tensor.

\*MAT\_157 is an anisotropic nonlinear elastoviscoplastic integrating principals anisotropic characteristics of the short fibers reinforced plastics for quasi-static and crash structural simulations.

The correlations on Faurecia beams are demonstrating a good level of correlation with the influence of the injection process.

This LS-Dyna anisotropic nonlinear elastoviscoplastic method improves simulation accuracy with a small computation time increase versus an isotropic method and a very good numerical stability without licence added cost.